Ni-Based Cr Alloys and Grain Boundaries Characterization

[1]Aezeden Mohamed and [2]Tarek Mohamed

[1](Faculty of Engineering and Applied Science, Memorial University, St. John's, NF, Canada, A1B 2X3)

[2](Waha Oil Company, Engineering Research Department, Tripoli, Libya,)

amohamed@mun.ca

ABSTRACT:

Three Ni-base alloys Hastelloy C22, Inconel 600, and Inconel 601 with carbon contents of 0.003, 0.05, and 0.3 wt. % respectively were used to investigate the effect of carbon on the morphology grain boundaries at constant heat treatment. From microstructural characterization and analysis, it was observed that the lowest carbon content resulted in planer character grain boundaries, the carbon content produced wavy grain boundaries and the highest carbon content produced saws-teeth grain boundaries. It is suggested that higher carbon contents result in the formation of occurred grain boundaries due to the formation of $M_{23}C_6$ morphology.

Keywords: *Boundary, Carbides, Grain, Hastelloy, Inconel, Morphology, Serration, Triangle*

I. INTRODUCTION

Ni-base alloys are widely used in space and marine environments due to their high strength, ductility and corrosion resistance. It is well documented that grain boundary serration occurs by the formation of precipitates along grain boundaries [1–6]. Investigators have found that, grain boundary serrations in stainless steel improve creep and fatigue properties of this alloy [5]. Furthermore, it has been found that in alloys 304 and 316 stainless steels, when grain boundaries are serrated the amount of carbides reduced and carbide precipitate shape changed from triangular to planar which has been proven to improve fatigue properties for those alloys [7]. In other studies [8,9] it was found that grain boundary serration occurs before carbides are precipitated on the grain boundaries. These studies also claim that when precipitation of carbides eventually occurs, planar carbides form along serrated boundaries while triangular carbides form along the unserrated boundaries. This contradicts previous reports that claim that grain boundary serration is due to precipitation of phases in the grain boundary serration. It has been found that the phase precipitated on grain boundaries in stainless steels are $M_{23}C_6$ type carbides [10-17]. Therefore, the main purpose of this study is to investigate the effect of carbon content on the morphology of grain boundary serration.

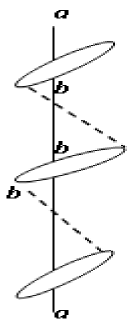

Figure 1Model shows grain boundary serration formation in stainless steel due to $M_{23}C_6$ precipitation, (a-a) grain boundary prior to formation of $M_{23}C_6$; (b-b), (c-c) serrated grain boundary after formation of $M_{23}C_6$ [10].

II. EXPERIMENTAL PROCEDURE

In order to investigate morphology of grain boundary serration in three kinds of Ni-base alloys are Hastelloy C22, Inconel 600, and Inconel 601, specimens were all solution heat treated at 1000°C for 1 hour followed by air cooling. Specimens were investigated under constant conditions using scanning electron microscopy and energy dispersive spectroscopy SEM-EDS.

Chemical compositions of the alloys are given in Table 1. To study grain boundary morphology with different carbon content, more than 5 specimens from each alloy were prepared and investigated under the same experimental conditions to confirm results.

Table 1 Nominal chemical composition of the three alloys

Chemical composition of Ni- alloys (wt.%)					
Alloy / Element	C	Fe	Mo	Cr	Ni
Haselloy C22	0.003	2.95	13.67	21.45	Bal.
Inconel 600	0.05	8.58	-	15.77	Bal.
Inconel 601	0.3	16.09	-	22.14	Bal.

Microstructural examination of Hastelloy C22 alloy (0.003%C) as shown in “Figure 2” reveals that more precipitates formed on grain boundaries. Also, the grain boundaries were essentially planar possibly because of the formation of the planer and spherical precipitates along these grain boundaries.

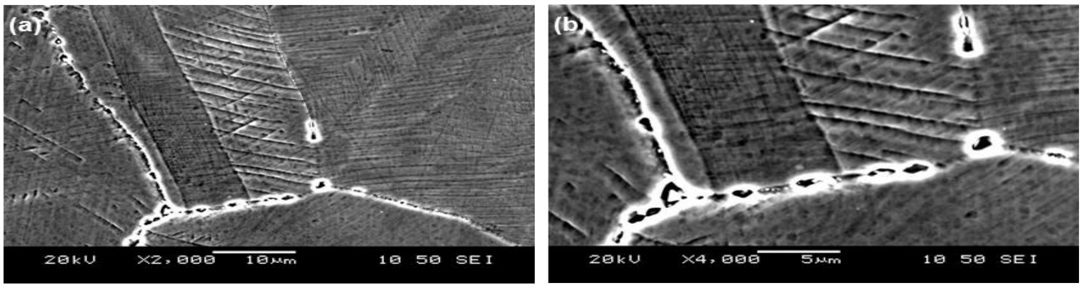

Figure 2 SEM images showing planer grain boundaries of Hastelloy C22 (a) at 2000 and (b) at 4000 magnification.

The morphology of the grain boundaries in Inconel 600 as shown in “Figure 3” is quite different from those for Hastelloy C22 as shown in “Figure 2”. In Inconel alloy 600, the grain boundaries have wavy appearance possibly due to the grain boundary formation of small amount of carbides. Further in Inconel 600 the grain boundaries are more rounded morphology compared to those in Hastelloy C22.

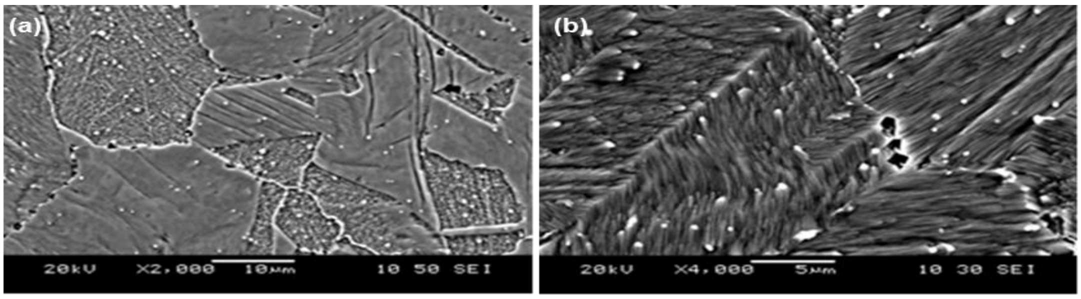

Figure 3 SEM images showing wavy grain boundaries of Inconel 600 (a) at 2000 and (b) at 4000 magnification.

In Inconel 601, it was observed that the grain boundaries are very distinct saw teeth shape like as shown in “Figure 4” and also the carbides precipitates within the grains are triangular in shape as shown in “Figure 5” and a single precipitate observed at 8000 magnification as shown in “Figure 5 b”. Further it was found that the grain boundaries are more visibly serrated in Inconel 601 than in Inconel 600 or Hastelloy C22.

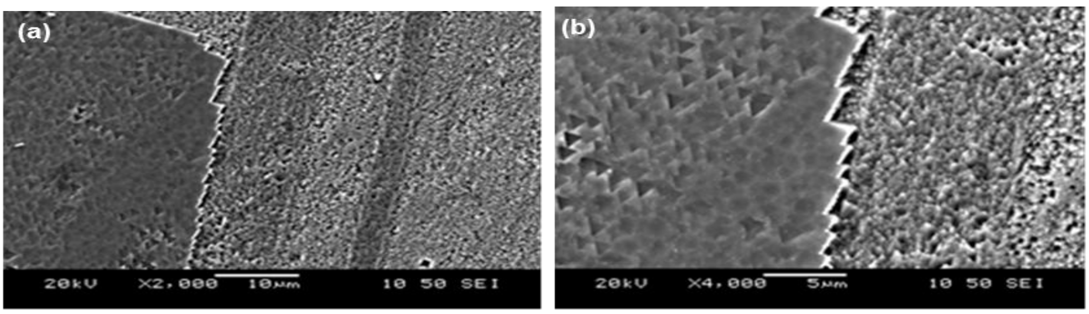

Figure 4 SEM images showing saw teeth and serrated grain boundaries of Inconel 601(a) at 2000 and (b) at 4000 magnification.

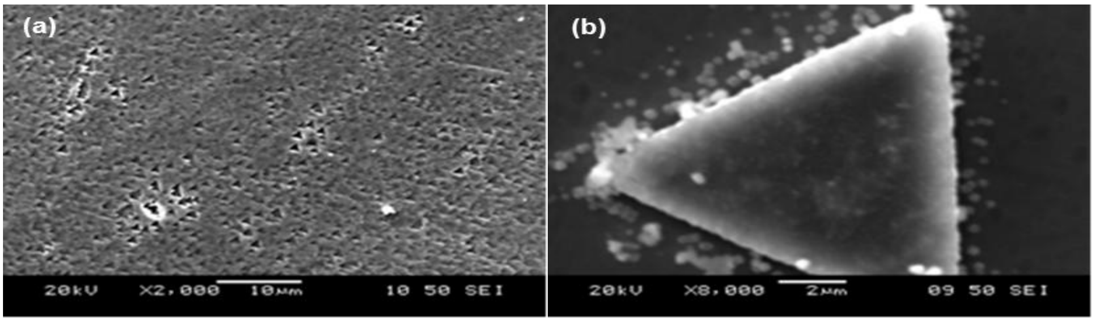

Figure 5 SEM images of triangle carbides precipitates in Inconel 601(a) at 2000 and (b) at 8000 magnification.

A major observation that Inconel 601 alloy which contains a significantly higher carbon content (C = 0.3%) showed the most visible within the grains and within grain boundaries serration. Also, Inconel 600 alloy (C = 0.05%) had more visibly serrated grain boundaries than Hastelloy C22 (C = 0.003%). Therefore, it can be concluded that the percentage of carbon composition possibly determines the morphology of the grain boundaries as well as the shape of grain boundaries precipitates. The higher the carbon content the more pronounced the grain boundary serration. Figure 6 general schematic diagram illustrate grain boundaries for the three alloys planar, wavy and saw teeth (a) Hastelloy C22 (b) Inconel 600 and (c) Inconel 601

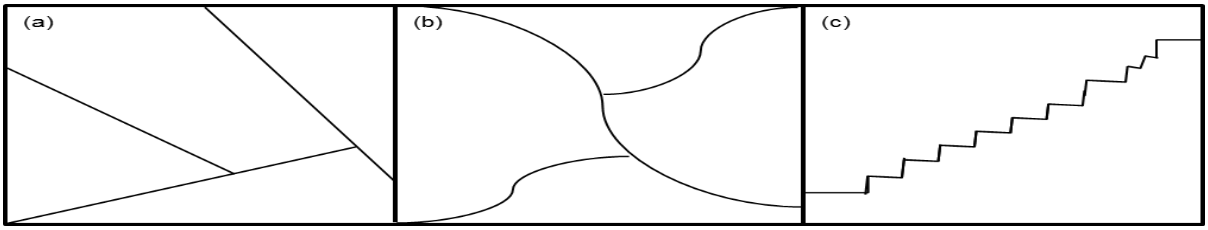

Figure 6 1Model shows grain boundaries planar serration, wavy, and saw teeth for (a) Hastelloy C22 (b) Inconel 600 and (c) Inconel 601 respectively.

Examination of the ternary Ni-Cr-Fe phase diagram [18] indicates that the major constituent phase in the three alloys considered is the γ phase. Further analysis done using computer program software JMatPro 4.0 shows that the Hastelloy C22 and Inconel 600 is the γ phase, whereas Inconel 601 show that the γ phase and M_7C_3 at temperature 1000°C for 1hour for three alloys as shown in “Figure 7”.

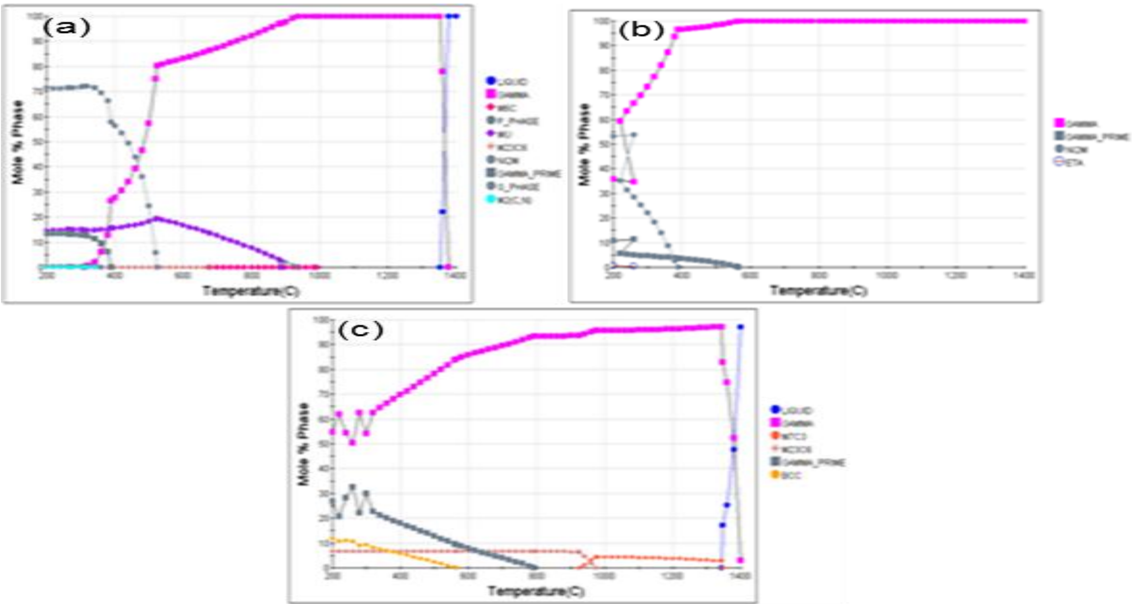

Figure 7 Show phase diagram of three Ni-base alloys solution treated at 1000°C for 1 hour followed by air cooled exhibited γ phase (a) Hastelloy C22, (b) Inconel 600 and (c) Inconel 601.

III. CONCLUSIONS

The study shows grain boundary morphology can be related to the amount of carbon present in nickel base alloys. Grain boundary serration becomes more pronounced with increasing carbon content. With increasing carbon content, grain boundary morphology changed from planar in Hastelloy C22 to serrate with rounded features in Inconel 600 alloy and to serrated with saw-teeth like appearance in Inconel 601.

REFERENCES

[1] K.J. Kim, J. Ginsztler, S.W. Nam, The Role of Carbon on the Occurrence of Grain Boundary Serration in an AISI 316 Stainless Steel during Aging Heattreatment, Materials Letters, 59:1439–1443, 2005.

[2] J.M. Larson and S. Floreen, Metallurgical Factors Affecting the Crack Growth Resistance of a Superalloy, Metallurgical Transactions A, 8: 51-53, 1977.

[3] T.M. Maccagno, A.K. Koul, J.-P. Immarigeon, L. Cutter, and R. Allem, Microstructure, Creep Properties, and Rejuvenation of Service-Exposed Alloy 713C Turbine Blades, Metallurgical Transactions A. 21: 3115-3125, 1990.

[4] M. Yamazaki and S. Hori, On the Baryon Mass Levels II, Progress of Theoretical Physics, 36:1035-1043:1966.

[5] M. Enomoto, H. Harada, M. Yamazakii , Calculation of γ'/γ Equilibrium Phase Compositions in Nickel-Base Superalloys by Cluster Variation Method, Calphad. 15:143–158, 1991.

[6] M. Tanaka, H. Iizuka, and F. Ashihara, Effects of Serrated Grain Boundaries on the Crack Growth in Austenitic Heat-Resisting Steels during high-temperature creep, Journal of Materials Science, 23:3827-3832, 1988.

[7] K.J. Kim, H. Hong, K. Min, S.W. Nam, Correlation between the Carbide Morphology and Cavity Nucleation in an Austenitic Stainless Steels under Creep-Fatigue, Materials Science and Engineering A, 387–389:531–535, 2004.

[8] K. S. Min, and S. W. Nam, Correlation between Characteristics of Grain Boundary Carbides and Creep–Fatigue Properties in AISI 321 Stainless Steel, Journal of Nuclear Materials, 322:91–97, 2003.

[9] H.U. Hong, S.W. Nam, Z. Crystallography Investigation on the Serrated Grain Boundary in an AISI 316 Stainless Steel, Journal of Nuclear Materials, 393:249–253, 2009.

[10] A.K. Koul and R. Thamburaj, Serrated Grain Boundary Formation Potential of Ni-Based Superalloys and Its Implications, Metallurgical Transactions A, 16:17-25, 1985.

[11] A.M. Donald, L.M. Brown, Grain Boundary Faceting in Cu-Bi Alloys, Acta Metallurgica, 27:59–61, 1979.

[12] T.E. Hsieh, R.W. Balluffi, Experimental Study of Grain Boundary Melting in Aluminum, Acta Metallurgica, 37:1637–1644, 1989.

[13] D.E. Luzzi, High-Resolution Electron Microscopy Observations of Faceted Grain Boundaries and Twins in Bismuth-Doped Copper, Ultramicroscopy, 37:180–181, 1991.

[14] T.G. Ference, R.W. Balluffi, Observation of a Reversible Grain Boundary Faceting Transition Induced by Changes of Composition, Technical Report, Massachusetts Inst. of Tech., Cambridge (USA), 22:1929–1930, 1988.

[15] M. Menyhard, B. Blum, C.J. McMahon, Grain Boundary Segregation and Transformations in Bi-doped Polycrystalline Copper, Acta Metallurgica, 37:549–557, 1989.

[16] J.R. Rellick, C. McMahon, H. Marcus, P. Palmberg, The Effect of Tellurium on lntergranular Cohesion in Iron, Metallurgical Transactions, 2:1492-1493, 1971.

[17] Chantal Loier and Jean-Yves Boos C. Loier, J.Y. Boos, The Influence of Grain Boundary Sulfur Concentration on the Intergranular Brittleness of Different Purities, Metallurgical Transactions A, 12:1222—1223, 1981.

[18] Donna Sue Plickert, Steve Starr, Karen Skiba, Patricia Eland, Jeff Fenstermaker, ASM Handbook, Alloy Phase Diagrams, 3:345–347, 1992.